

# Experimental demonstration of localized Brillouin gratings with low off-peak reflectivity established by perfect Golomb codes

Yair Antman,<sup>1</sup> Lior Yaron,<sup>2</sup> Tomi Langer,<sup>2</sup> Moshe Tur,<sup>2</sup> Nadav Levanon,<sup>2</sup> and Avi Zadok<sup>1,\*</sup>

<sup>1</sup>Faculty of Engineering, Bar-Ilan University, Ramat-Gan 52900, Israel

<sup>2</sup>School of Electrical Engineering, Faculty of Engineering, Tel-Aviv University, Tel-Aviv 69978, Israel

\*Corresponding author: Avinoam.Zadok@biu.ac.il

Received August 12, 2013; accepted September 22, 2013;

posted October 3, 2013 (Doc. ID 195615); published November 11, 2013

Dynamic Brillouin gratings (DBGs), inscribed by comodulating two writing pump waves with a perfect Golomb code, are demonstrated and characterized experimentally. Compared with pseudo-random bit sequence (PRBS) modulation of the pump waves, the Golomb code provides lower off-peak reflectivity due to the unique properties of its cyclic autocorrelation function. Golomb-coded DBGs allow the long variable delay of one-time probe waveforms with higher signal-to-noise ratios, and without averaging. As an example, the variable delay of return-to-zero, on-off keyed data at a 1 Gbit/s rate, by as much as 10 ns, is demonstrated successfully. The eye diagram of the reflected waveform remains open, whereas PRBS modulation of the pump waves results in a closed eye. The variable delay of data at 2.5 Gbit/s is reported as well, with a marginally open eye diagram. The experimental results are in good agreement with simulations. © 2013 Optical Society of America

OCIS codes: (060.4370) Nonlinear optics, fibers; (190.2055) Dynamic gratings; (290.5900) Scattering, stimulated Brillouin.

<http://dx.doi.org/10.1364/OL.38.004701>

The all-optical variable delay of broadband waveforms has raised much interest in recent years [1]. In particular, optical fibers are regarded as an attractive platform for variable-delay demonstrations, due to the potential incorporation of such setups in optical communication and microwave-photonic systems [2,3]. A well-accepted figure of merit for variable-delay setups is their *delay-bandwidth product*: the product of maximum attainable delay variation and the maximum bandwidth that is supported, subject to constraints on the waveform quality. A delay-bandwidth product of nearly 100,000 was obtained using wavelength conversion and propagation in long sections of dispersive fibers [4,5]. Alternatively, “slow light” setups, such as those based on stimulated Brillouin scattering (SBS), can be realized in shorter fiber sections with only a modest change in center wavelength [2,3]. However, the delay-bandwidth product of SBS slow light is fundamentally restricted to the order of unity [6,7].

Over the past five years, dynamic Brillouin gratings (DBGs) in polarization-maintaining (PM) fibers were implemented in numerous sensing and all-optical signal-processing applications [8–21]. A DBG is associated with the acoustic wave that is formed by the SBS interaction between two counter-propagating optical “writing” pump waves, which are copolarized along one principal axis of the PM fiber. The strength of the DBG at a given position is proportional to the temporal cross correlation between the complex envelopes of the two writing waves at that point, windowed over twice the Brillouin lifetime  $\tau$  of  $\sim 5$  ns [17,22,23]. The gratings can be interrogated by a third, optical probe wave, polarized along the orthogonal principal axis. Due to the large birefringence of PM fibers, the frequency of the probe wave must be detuned from those of the pumps, typically by a few tens of gigahertz.

The spatial locations of the DBGs are controlled through modifications to the writing waves, effectively

implementing “movable mirrors.” Hence, DBGs are being considered as a new candidate platform for the realization of variable, all-optical delays. The delay of broadband waveforms requires that the DBGs are spatially confined. Stationary and localized DBGs can be realized through synchronized frequency modulation of the two writing waves [14], or through their phase modulation by the output of a chaotic system [22], or by a pseudo-random bit sequence (PRBS) [12,17,18]. In all of the above methods, the cross correlation between the envelopes of the two writing waves is confined to discrete and narrow peaks.

PRBS phase coding has been successfully implemented in high-resolution Brillouin sensing [18], microwave-photonic filters [12], and also in the variable delay of probe pulses [17]. However, the optical signal-to-noise ratio (OSNR) of reflected, delayed waveforms was severely degraded by reflections from residual, off-peak DBGs (“coding noise”). OSNR levels were unacceptably low, unless delay variations were restricted to fractions of  $\tau$  or averaging over numerous repetitions of identical probe patterns was mandated [17].

In a recent publication [24], we proposed the application of advanced phase sequences, known as “perfect Golomb codes” [25], to the modulation of the DBG writing waves. The cyclic autocorrelation function of the codes of this class assumes off-peak values of exactly zero [25]. Previous analysis had shown that due to this property, the comodulation of the writing waves by a perfect Golomb code could lead to localized DBGs with substantially reduced off-peak reflectivity, compared with that of PRBS modulation-inscribed DBGs [24]. Consequently, a longer delay of probe waveforms, with higher OSNRs and without averaging, had been predicted. A corresponding experiment, however, has not yet been reported.

In this work, we present an experimental demonstration of DBGs driven by Golomb-coded pump waves.

We characterize their use as movable mirrors in a variable-delay line and compare their performance with that of DBGs written by PRBS-coded pumps. Return-to-zero (RZ), on-off keyed (OOK) PRBS probe waves at 1 Gbit/s rate were delayed successfully by as much as 10 ns, corresponding to a delay-bandwidth product of 10. The OSNR provided by the Golomb coding of the DBGs was sufficient to obtain reflected probe sequences with an open eye diagram, whereas the eye diagram obtained using the PRBS-coded writing waves appeared closed. An extension of the experiment to the delay of RZ, OOK PRBS probe waves at 2.5 Gbit/s (delay-bandwidth product of 25) resulted in an eye diagram that was only marginally open.

The experimental setup is illustrated in Fig. 1. A distributed feedback (DFB) laser at 1550 nm wavelength was the source of the two writing SBS pump waves. Light at the DFB output was modulated by an external electro-optic phase modulator, driven by an arbitrary waveform generator (AWG) that was programmed to either a Golomb code or a PRBS at 5 Gbit/s. The longitudinal extent of the DBGs induced by this pump modulation rate is 2 cm. The Golomb code  $a_n$  was of length  $N = 63$ . The phases of elements  $n = \{1\ 2\ 3\ 4\ 5\ 7\ 8\ 9\ 10\ 13\ 14\ 15\ 17\ 19\ 20\ 25\ 27\ 28\ 29\ 33\ 34\ 36\ 37\ 39\ 42\ 46\ 49\ 50\ 53\ 55\ 57\}$  in the Golomb code equal  $\text{acos}(-62/64)$ , whereas the phases of all other elements are set to zero [24]. The code was repeated every  $N$  bits. The cyclic autocorrelation of  $a_n$ ,

$$R_N(l) \equiv \sum_{n=n_0-N}^{n_0} a_n a_{n-l}^*, \quad (1)$$

is zero for any offset  $l \neq 0$  and any starting point  $n_0$ . The magnitude of the AWG output waveform was amplified to carefully match  $V_\pi$  of the modulator.

The phase-coded optical signal was split into two branches of writing pumps 1 and 2. Pump 1 was delayed in a 50-m-long fiber path imbalance, which is necessary

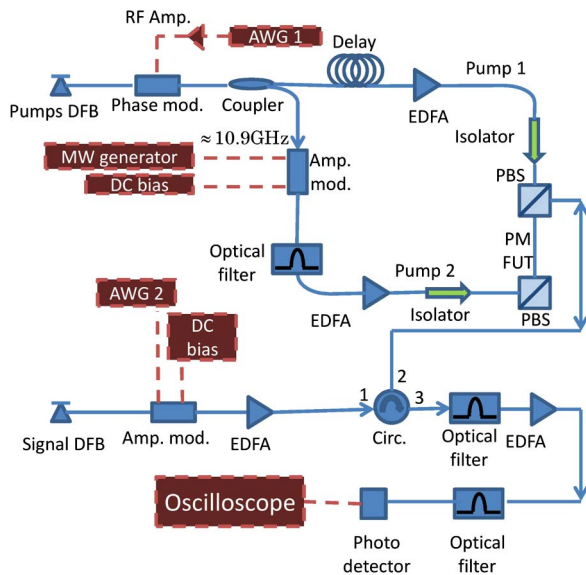


Fig. 1. Experimental setup for generation and interrogation of stationary and localized DBGs. MW, microwave.

for fine-tuning the location of the DBG [17,18]. Pump 1 was then amplified by an erbium-doped fiber amplifier (EDFA) to an optical power of 2 W and launched along the fast axis of a fiber under test (FUT) through a polarization beam splitter (PBS). Pump 2 passed through an electro-optic amplitude modulator that was biased for carrier suppression and driven by a sine wave at the Brillouin frequency shift of the fiber  $\nu_B \sim 10.86$  GHz. An optical bandpass filter was used to retain a single modulation sideband, shifted in frequency from pump 1 by  $\nu_B$ . Pump 2 was then amplified by a second EDFA to an optical power of 500 mW and launched along the fast axis from the opposite end of the FUT through a second PBS.

A second DFB laser was used as the source of the readout probe waves. Its frequency was tuned for maximum reflectance from the DBG for signals polarized along the slow axis [8]:

$$\nu_{\text{sig}} = \nu_2 + \Delta\nu = \nu_2 + (\Delta n_g/n)\nu_2. \quad (2)$$

In Eq. (2),  $\nu_{\text{sig}}$  and  $\nu_2$  are the optical carrier frequencies of the probe signal and pump 2, respectively;  $\Delta n_g \ll 1$  denotes the difference between the group indices along the fast and slow axes of the PM fiber due to birefringence; and  $n$  is the group index along the fast axis. The frequency difference  $\Delta\nu$  was 48 GHz. The probe wave, serving as the signal to be delayed, was amplitude modulated by a RZ, OOK PRBS pattern, amplified, and launched along the slow axis of the FUT toward the DBG. The PRBS pattern was repeated at 10% duty cycle and amplified to an average power of 500 mW. Hence the peak power of the signal wave PRBS “On” pulses was 10 W. The FUT itself was stretched along a metal rod, in order to reduce temperature and strain variations (and consequently, reduce spatial variations of  $\nu_B$  and  $\Delta n_g$ ).

Probe waves reflected from the DBG propagated back through a circulator and were filtered by an optical bandpass filter, tuned to  $\nu_2 - \nu_B$ . The filter rejected residual leakage and reflections at the frequencies of the pump waves and the incoming readout probe. The reflectivity of the 2-cm-long DBG was very weak: only  $-64$  dB. The reflected waveforms were therefore amplified to a peak power level of 1 mW by another EDFA and filtered again by a 4-GHz-wide optical bandpass filter to remove out-of-band amplified spontaneous emission (ASE). Finally, the reflected probe waves were detected by a photodetector, and the photocurrents passed through a 4-GHz-wide electrical low-pass filter and were sampled by an oscilloscope at a rate of 80 Gsamples/s.

The SNR of reflected probe waves can be estimated as follows: the thermal and electrical noise of the photodetector, integrated over the bandwidth of interest of 4 GHz, is equivalent to an input optical power level of  $1.5 \mu\text{W}$ . The power of ASE from the EDFA at the detection branch (gain of 27 dB, noise figure of 6 dB), within the optical filter bandwidth, is  $1.1 \mu\text{W}$ . Both the detector noise and the noise due to beating between ASE and the reflected probe field are therefore considerably weaker than the mean photocurrent due to the amplified, reflected probe pattern. The power levels of the residual reflections of the pump and the input probe waves at the

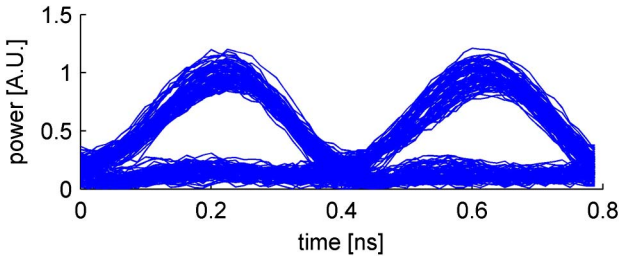


Fig. 2. Measured eye diagrams of 2.5 Gbit/s RZ, OOK PRBS probe waves, with the DBG temporarily replaced by an equivalent attenuator of 64 dB.

optical bandpass filter output were below  $-25$  dBm. The OSNR of the reflected probe sequences is therefore expected to be limited by coding noise [25]. For verification, the DBG in the probe path was temporarily replaced by a fixed equivalent attenuator of 64 dB and an output eye diagram was recorded (Fig. 2). The quality of the output waveform was very good.

The DBGs were first characterized using single, isolated probe pulses that were 200 ps long. Figure 3 shows the relative power reflected from the DBG as a function of time. The trace can be regarded as an “impulse response” of the localized DBGs. The average off-peak reflectivity of the Golomb-coded DBG is lower than that of the PRBS-coded one by a factor of 3.1. The corresponding ratio predicted by simulation is about 4 [24].

The impulse response of Golomb-coded DBGs for several slightly different writing sequence clock rates is shown in Fig. 4. As described in detail in [18], the separation between neighboring correlation peaks is  $0.5Nv_gT$ , with  $v_g$  the group velocity of light in the fiber and  $T$  the duration of a single coding symbol. Due to the path imbalance between the two pump branches, a high-order correlation peak could be scanned along the FUT by slightly tuning the rate of the coding sequence. Clock rate variations in the range of 4.81–5.25 GHz effectively moved the DBG along the entire 1-m-long FUT, introducing delay variations of reflected probe pulses by up to 10 ns.

Figure 5 shows the eye diagrams of delayed probe waves, modulated by RZ, OOK PRBS at 1 Gbit/s. The waveforms were reflected from Golomb-coded (top)

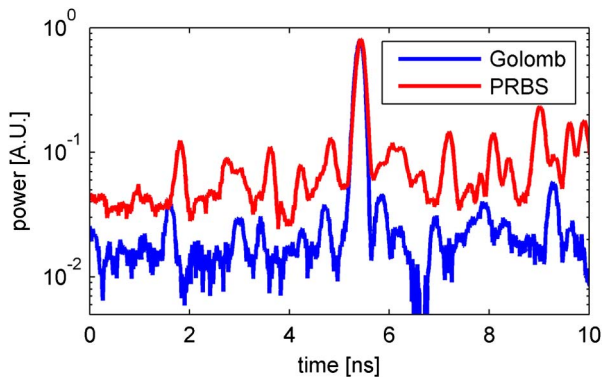


Fig. 3. Relative reflected power from stationary and localized DBGs as a function of time (“impulse response”). The interrogating probe waveform was a single, isolated pulse of 200 ps duration. Blue, Golomb-coded DBG; red, PRBS-coded DBG.

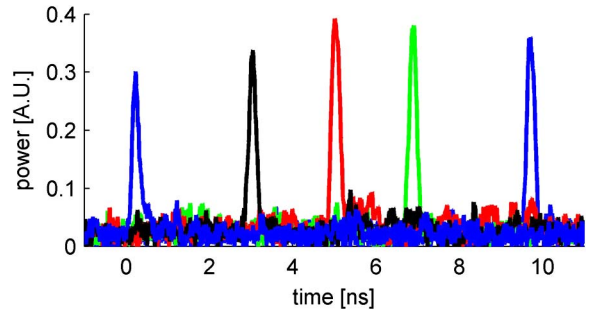


Fig. 4. Variable delay of single, isolated probe pulses using Golomb-coded stationary and localized DBGs.

and PRBS-coded (bottom) DBGs. The pumps were modulated at 5 Gbit/s. An open eye is obtained using Golomb coding, whereas the eye diagram for the PRBS-coded DBG is closed. The corresponding simulated eye diagrams are shown in Fig. 6 [24]. Good agreement between experiment and simulations is evident. The results

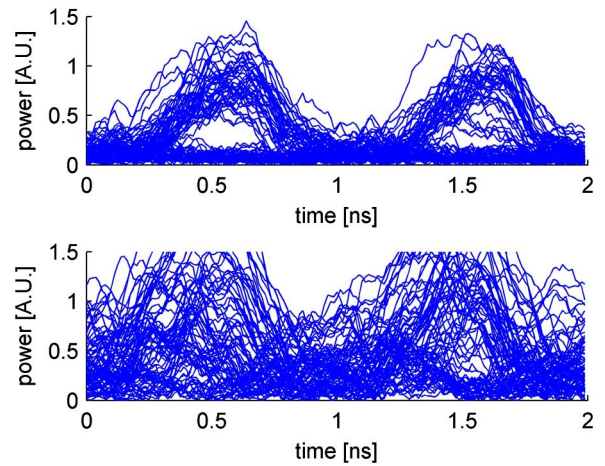


Fig. 5. Measured eye diagrams of 1 Gbit/s RZ, OOK PRBS probe waves, reflected from DBGs that were written by Golomb code modulation of the pump waves (top) and PRBS modulation (bottom). The pump modulation rate was 5 Gbit/s.

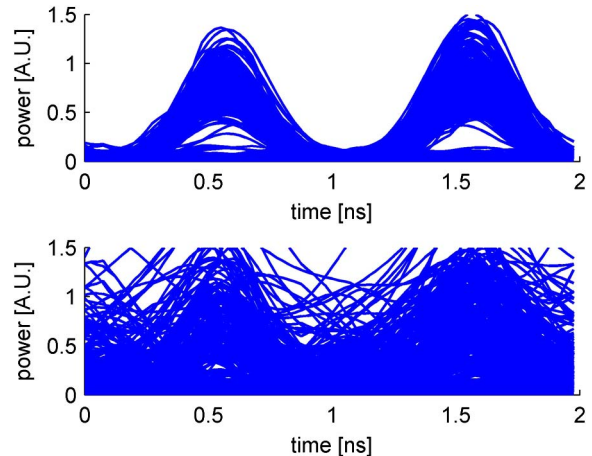


Fig. 6. Simulated eye diagrams of 1 Gbit/s RZ, OOK PRBS probe waves, reflected from DBGs that were written by Golomb code modulation of the pump waves (top) and PRBS modulation (bottom). The pump modulation rate was 5 Gbit/s.

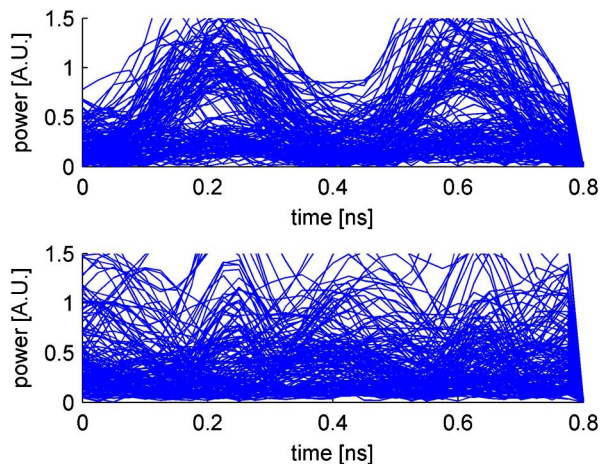


Fig. 7. Measured eye diagrams of 2.5 Gbit/s RZ, OOK PRBS probe waves, reflected from DBGs that were written by Golomb code modulation of the pump waves (top) and PRBS modulation (bottom). The pump modulation rate was 5 Gbit/s.

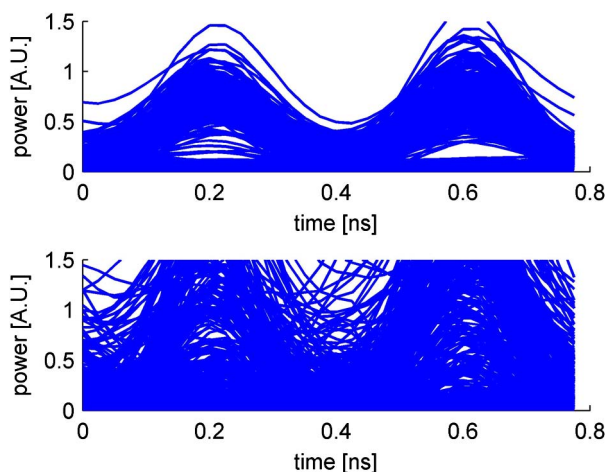


Fig. 8. Simulated eye diagrams of 2.5 Gbit/s RZ, OOK PRBS probe waves, reflected from DBGs that were written by Golomb code modulation of the pump waves (top) and PRBS modulation (bottom). The pump modulation rate was 5 Gbit/s.

indicate that the coding noise of the Golomb-encoded DBG is lower than that of the PRBS-inscribed one. Figures 7 and 8 show the experimental and simulated eye diagrams of reflected RZ, OOK PRBS probe data at 2.5 Gbit/s. The Golomb- and PRBS-coded DBGs were the same as those in Figs. 5 and 6. The eye diagram obtained using the Golomb-coded DBG is only marginally open at this data rate.

In conclusion, localized and stationary DBGs were generated successfully using Golomb-coded pumps. The off-peak reflectivity of these gratings is lower than that of PRBS-coded DBGs, as predicted by simulations. The application of DBGs to variable delay of data was demonstrated. RZ, OOK PRBS data at 1 Gbit/s was delayed by 10 ns, with an OSNR that was sufficiently high to retain an open eye diagram. This result could not be obtained using PRBS-coded DBGs. The delay-bandwidth product of 10 is an order of magnitude larger than those of broadband SBS slow light-based setups. The results

demonstrate the added value of advanced radar-based techniques in fiber-optic signal processing. Currently, a major drawback of the technique is the weak reflectivity of wideband (and therefore short) DBGs in standard silica PM fibers, as low as  $-64$  dB in our case, which required the use of high power levels of the pump waves and the input probe. Higher reflectivity can be obtained using SBS in nonsilica fibers [26].

The work of Yair Antman and Avi Zadok was supported in part by the Chief Scientist Office, the Israeli Ministry of Industry, Trade and Labor, through the KAMIN program. The work of Lior Yaron, Tomi Langer, and Moshe Tur was supported in part by the Israel Science Foundation (ISF, Grant No. 1380/12). This work was realized in part within the collaborative framework of the EU COST Action TD1001 OFSESA.

## References

1. R. W. Boyd and D. J. Gauthier, *Progress in Optics*, E. Wolf, ed. (Elsevier, 2002), Vol. 43, pp. 497–530.
2. L. Thevenaz, *Nat. Photonics* 2, 474 (2008).
3. A. Zadok, A. Eyal, and M. Tur, *Appl. Opt.* 50, E38 (2011).
4. Y. Wang, C. Yu, L. Yan, A. E. Willner, R. Roussev, C. Langrock, M. M. Fejer, J. E. Sharping, and A. Gaeta, *IEEE Photon. Technol. Lett.* 19, 861 (2007).
5. Y. Dai, Y. Okawachi, A. C. Turner-Foster, M. Lipson, A. L. Gaeta, and C. Xu, *Opt. Express* 18, 333 (2010).
6. R. W. Boyd and P. Narum, *J. Mod. Opt.* 54, 2403 (2007).
7. J. B. Khurgin, *Slow Light—Science and Applications* (CRC Press, 2009), pp. 293–320.
8. K. Y. Song, W. Zou, Z. He, and K. Hotate, *Opt. Lett.* 33, 926 (2008).
9. Y. Dong, X. Bao, and L. Chen, *Opt. Lett.* 34, 2590 (2009).
10. W. Zou, Z. He, and K. Hotate, *Opt. Express* 17, 1248 (2009).
11. S. Chin, N. Primerov, and L. Thevenaz, *IEEE Sens. J.* 12, 189 (2012).
12. J. Sancho, N. Primerov, S. Chin, Y. Antman, A. Zadok, S. Sales, and L. Thevenaz, *Opt. Express* 20, 6157 (2012).
13. S. Chin, N. Primerov, and L. Thevenaz, *Proceedings of the 36th European Conference on Optical Communication (ECOC, 2010)*, Torino, Italy, 2010.
14. W. Zou, Z. He, K. Y. Song, and K. Hotate, *Opt. Lett.* 34, 1126 (2009).
15. K. Y. Song, K. Lee, and S. B. Lee, *Opt. Express* 17, 10344 (2009).
16. D.-P. Zhou, Y. Dong, L. Chen, and X. Bao, *Opt. Express* 19, 20785 (2011).
17. Y. Antman, N. Primerov, J. Sancho, L. Thevenaz, and A. Zadok, *Opt. Express* 20, 7807 (2012).
18. A. Zadok, Y. Antman, N. Primerov, A. Denisov, J. Sancho, and L. Thevenaz, *Laser Photonics Rev.* 6, L1 (2012).
19. M. Santagiustina, S. Chin, N. Primerov, L. Ursini, and L. Thevenaz, *Sci. Rep.* 3, 1594 (2013).
20. L. Ursini and M. Santagiustina, *IEEE Photon. Technol. Lett.* 25, 1347 (2013).
21. H. G. Winful, *Opt. Express* 21, 10039 (2013).
22. M. Santagiustina and L. Ursini, *Opt. Lett.* 37, 893 (2012).
23. R. W. Boyd, *Nonlinear Optics*, 3rd ed. (Academic, 2008).
24. Y. Antman, N. Levanon, and A. Zadok, *Opt. Lett.* 37, 5259 (2012).
25. S. W. Golomb, *IEEE Trans. Aerosp. Electron. Syst.* 28, 383 (1992).
26. K. Y. Song, K. S. Abedin, K. Hotate, M. González Herráez, and L. Thevenaz, *Opt. Express* 14, 5860 (2006).